Intramolecular Vibrational Excitation of Unfolding Reactions in Zn^{II}-Substituted and Metal-Free Cytochromes *c*: Activation Enthalpies from Integrated Fluorescence Stokes Shift and Line Shape Excitation Profiles

Kenneth J. Barns,[†] Sanela Lampa-Pastirk, Kevin L. Dillman, and Warren F. Beck*

Department of Chemistry, Michigan State University, East Lansing, Michigan 48824

Received: April 29, 2008; Revised Manuscript Received: September 8, 2008

We have employed continuous-wave fluorescence spectroscopy to observe the light-induced formation of partially unfolded states of Zn^{II}-substituted and metal-free (or free-base) cytochrome *c* (ZnCytc and fbCytc, respectively). In these experiments, the intrinsic porphyrin chromophore provides a vibrational excitation to the protein structure via intramolecular vibrational redistribution of the excess vibronic energy above the first excited singlet state. As the excitation light source is tuned, the fluorescence spectrum of both systems exhibits steplike transitions of the integrated Stokes shift, vibronic structure, and line width that mark apparent activation enthalpy barriers for structural transitions of the protein from the native state to a set of at least three partially unfolded states. The vibronic structure of the ZnCytc spectrum reports the exchange of the Zn^{II} ion's native H18 and M80 axial ligands with non-native ligands as the excitation wavenumber is scanned through the three barriers. The metal ion's axial ligands contribute substantially to the stability of ZnCytc; the activation enthalpies for the corresponding transitions in fbCytc are one-third of those in ZnCytc. A comparison of the present results from ZnCytc with those obtained previously with picosecond time-resolved methods [Lampa-Pastirk and Beck, *J. Phys. Chem. B* **2006**, *110*, 22971−22974] indicates that the vibrationally excited protein structure propagates along an unfolding pathway from the native state that specifically populates the three states in order of their activation enthalpies. The excitation−wavenumber profile of the fluorescence line width is markedly inconsistent with a Maxwell−Boltzmann distribution over the three states. These results contrast with the general expectation of the protein-folding funnel hypothesis that a distribution of intermediate structures should result from the diffusive propagation of a nonequilibrium protein structure.

1. Introduction

The rapid folding of proteins into functional structures involves a diffusive propagation over a funnel-shaped potential energy surface leading to formation of the native structure at the global minimum.[1−8] This hypothesis inherently suggests that an ensemble of folding trajectories exists between the unfolded and native states,[9] so a range of intermediate configurations should be transiently populated during the folding reaction. Further, because of the low local activation barriers that confine the native structure,[5] misfolded proteins and alternative conformations may arise spontaneously through thermally activated processes.

A significant test of the protein-folding funnel hypothesis is to observe the propagation of an ensemble of protein molecules following a *vertical* excitation, a change in enthalpy on a time scale that is short compared to the characteristic time scale for fluctuations of the native structure. We reported recently that such an excitation is obtained via intramolecular vibrational redistribution (IVR) processes from the radiationless decay and/or vibrational relaxation of an intrinsic electronic chromophore.[10] With excitation of the S_1 state at the wavenumber of the 0−0 vibronic transition in the Q absorption band (see Figure 1), the dynamic Stokes shift of the time-resolved fluorescence spectrum observed in Zn^{II}-substituted cytochrome *c* (ZnCytc) is a conventional, unidirectional shift to the red (see Figure 2). This signal accompanies a polar solvation response[11] of the protein structure to the ground-to-excited-state change in the Zn^{II}−porphyrin's dipole moment. The two exponential relaxation components are assigned to the fluctuations of the hydrophobic core and solvent-contact regions of the protein, the latter on the basis of its sensitivity to the external solvent

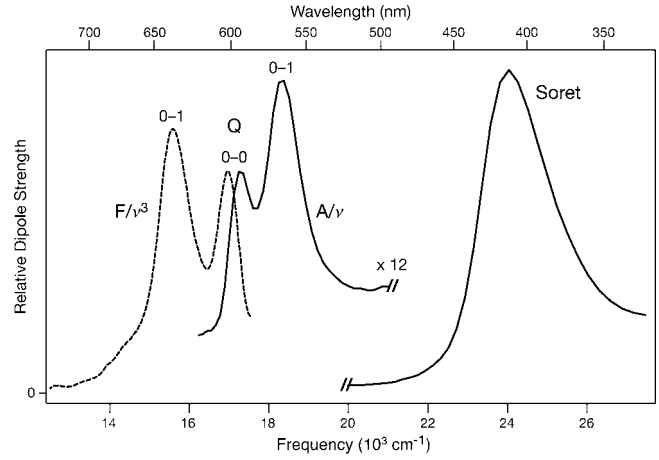

Figure 1. Continuous-wave absorption (A/ν, solid curve) and fluorescence (F/ν^3, dashed curve) dipole strength spectra from Zn^{II}-substituted cytochome *c* (ZnCytc) at 22 °C. The fluorescence spectrum was recorded with the excitation monochromator tuned to the wavenumber of the 0−0 vibronic transition, where the absorption and fluorescence dipole strength spectra cross. The 0−0 and 0−1 peaks in the absorption and fluorescence spectra are marked.

* Corresponding author: e-mail beckw@msu.edu; Fax 517-353-1793.
[†] Current address: Department of Chemistry, University of Wisconsin, Madison, WI 53706.

10.1021/jp803756n CCC: $40.75
Published on Web 10/28/2008

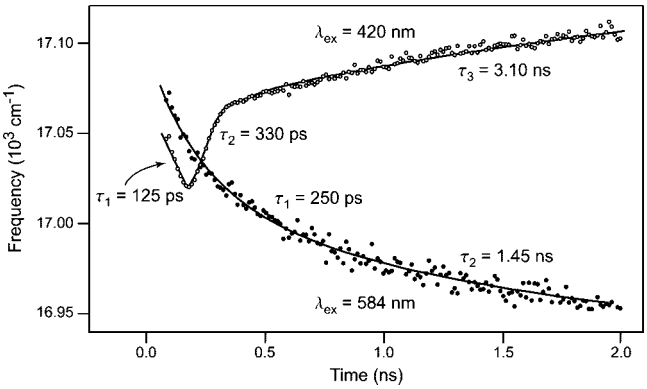

Figure 2. Dynamic Stokes shift of the fluorescence spectrum from ZnCytc in water at 22 °C: with excitation at 420 nm, in the Soret absorption band, or with excitation at 584 nm, in the Q absorption band at the 0−0 vibronic transition. The wavenumber for the maximum of the 0−0 peak in the time-resolved fluorescence spectrum is plotted in each case as a function of the time delay following the 10 ps excitation pulse. From ref 10.

viscosity, that accompany diffusive sampling of the native minimum.[12] In contrast, when ZnCytc is excited in the Soret absorption band, a bidirectional dynamic Stokes shift is observed; an initially fast shift of the time-resolved fluorescence spectrum to the red is followed by a slower, biexponential shift to the blue that persists throughout the fluorescence time window.

The unusual dynamic Stokes shift observed in ZnCytc with Soret band excitation arises from a change in the structure of the protein medium surrounding the intrinsic Zn^{II}−porphyrin that is triggered by the IVR-mediated transfer of vibrational energy from the porphyrin to the protein. Because the continuous-wave fluorescence spectrum exhibits a comparable shift to the blue as ZnCytc undergoes a thermal unfolding transition,[13] we suggested that Soret band excitation directly prepares the transition state for the unfolding of ZnCytc to an unfolded or partially unfolded state. The excess vibronic energy above the S_1 state (see Figure 3) is transferred to the protein structure as a vibrational excitation on the 2 ps or shorter time scale. Because the IVR time scale is an order of magnitude shorter than that for collisional energy transfer to the surrounding water solvent,[14−16] the protein propagates structurally at an excited vibrational level for ∼20 ps. This interval is apparently long enough for the protein to pass over the transition-state barrier that confines the native state and leads to the formation of unfolded or partially unfolded states. The product states are formed under solution conditions that favor formation of the native state, so it is expected that they refold on a time scale that is long compared to the prompt fluorescence window.[10] This conclusion is consistent with the results of picosecond transient grating experiments with ferricytochrome *c* (FeCytc), which detected the formation of long-lived nonequilibrium conformational states after Soret band excitation.[17]

As an initial characterization of the activation-enthalpy profile for the unfolding reactions from the native state, we present in this contribution a characterization of the continuous-wave fluorescence spectrum from ZnCytc and metal-free (or free-base) cytochrome *c* (fbCytc) as a function of the wavenumber of the excitation light source. By scanning the excitation source above the wavenumber of the 0−0 absorption transition, we vary the excess vibronic energy with which the S_1 state is prepared. The enthalpy of activation that yields a new structure from the native state is marked by a shift of the fluorescence spectrum, either to the red or blue, as the protein assumes a

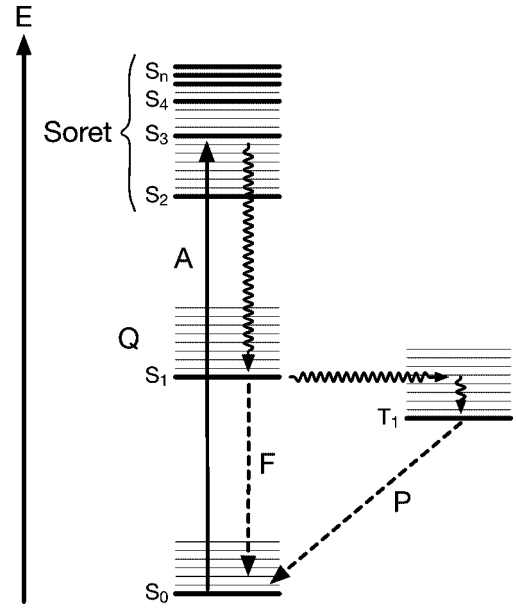

Figure 3. Photophysical processes in metal-free (or free-base) and Zn^{II} porphyrins. The vibronic energy levels are indicated schematically by horizontal lines. An absorption transition (A) into the Soret band is marked by the solid vertical arrow. The nonradiative vibrational-relaxation and intersystem-crossing processes that occur subsequently are indicated by downward and horizontal wavy arrows, respectively. The ground-state recovery paths via the radiative fluorescence (F) and phosphorescence (P) processes are indicated by dashed arrows.

new structure around the porphyrin chromophore. Figure 2 indicates that the time-integrated fluorescence spectrum obtained with Soret band excitation is slightly blue-shifted with respect to that observed with Q band excitation; the initial red and blue phases of the dynamic Stokes shift essentially cancel each other, but the subsequent shift to the blue that persists to the end of the fluorescence time scale results in a net shift of the integrated spectrum to the blue. Figure 1 shows that the absorption dipole strength is continuous (nonzero) from the origin of the Q band all the way through the Soret band, which prepares the S_2 state and higher singlet states (S_n), so it is possible to excite the protein over a considerable range of vibrational energies. The energy range is comparable to previous estimates for the barriers for folding and/or unfolding of FeCytc.[18,19]

The results show that the fluorescence spectra of ZnCytc and fbCytc exhibit a sequence of relatively sharp step transitions of the integrated fluorescence Stokes shift at several excitation wavenumbers between the Q and Soret bands. The ZnCytc spectrum also exhibits a set of step transitions in the vibronic structure that report the release of the native H18 and M80 ligands and the binding of non-native axial ligands to the Zn^{II} ion. These findings support the conclusion that intramolecular vibrational excitation of the protein structure drives the rapid formation of at least three partially unfolded states. A comparison of the sequence of integrated Stokes shifts to the time-resolved fluorescence Stokes shift observed with excitation in the Soret band suggests that the partially unfolded structures are specifically populated along a pathway. This result appears to be distinct from the distribution of structures anticipated by the protein-folding funnel hypothesis.

2. Experimental Section

2.1. Sample Preparation. ZnCytc and fbCytc were prepared from horse-heart FeCytc using the procedure developed in the Vanderkooi laboratory.[20] Liquid anhydrous hydrogen fluoride

(Linde) was employed as the demetalating agent; the reaction was run on a home-built gas-handling system in Teflon reaction vessels. Metal reconstitution of the fbCytc product with Zn^{II} was performed in the presence of a 10-fold molar excess of zinc acetate (Sigma 379786-5G, 99.999%). The extent of the demetalation and metal-reconstitution reactions was monitored spectrophotometrically; the starting FeCytc and product fbCytc or ZnCytc species are easily distinguished from each other in terms of the number and position of bands in the Q-band region of the absorption spectrum.

ZnCytc and fbCytc product solutions were subsequently worked up using methods described by Winkler and co-workers[21] and by Kostić and co-workers.[22] After desalting, the protein was isolated by cation-exchange chromatography, first on a Whatman CM-52 column and optionally then on a Mono-S 4.6/100 PE FPLC column (GE Healthcare Life Sciences). Fractions corresponding to ZnCytc or fbCytc were equilibrated with a 25 mM sodium phosphate buffer solution at pH 6.9 by repeated concentration using an Amicon Centriprep ultrafilter and dilution with the buffer solution. After a final ultrafiltration step, the product was analyzed on a Superdex 75 FPLC gel-filtration column (GE Healthcare Life Sciences). The eluent was monitored simultaneously at 280 and 420 nm. The gel-filtration column was calibrated using a solution of low-molecular-weight protein standards (GE Healthcare Life Sciences, LMW standards kit). The chromatograms (not shown) indicate that the porphyrin binding fractions correspond exclusively to monomeric cytochrome *c* species and that the samples are free of low-molecular-weight peptide fragments. For use in fluorescence experiments, the ZnCytc and fbCytc samples were diluted in the pH 6.9 buffer solution to obtain an absorbance of 0.12 for the Q-band maximum.

2.2. Continuous-Wave Absorption and Fluorescence Spectroscopy. Absorption spectra were acquired with a Hitachi U-2000 spectrophotometer (2 nm band-pass). Fluorescence spectra were obtained with a home-built spectrofluorimeter consisting of an Jobin-Yvon AH10 100 W tungsten−halogen light source, a Jobin-Yvon H10 excitation monochromator (4 nm bandpass), an Acton Research SP-150 emission spectrograph (2 nm bandpass), and a Jobin-Yvon Symphony charge-coupled device (CCD) detector. The CCD detector employs a liquid nitrogen cooled, back-illuminated, 2000 × 800 pixel silicon detector chip (EEV corporation). A 300 groove/mm diffraction grating (500 nm blaze wavelength) is mounted in the emission spectrograph, so a 270 nm spectral range is imaged over 2000 vertically binned channels on the CCD detector chip. The spatially integrated power of the excitation beam, as estimated using a Newport model 835 power meter and a model 818-SL silicon photodiode detector, was 20 μW at 530 nm. Fluorescence emission spectra were acquired as the average of typically 20 1 min exposures of the CCD detector. The sample cuvette was held in a Quantum Northwest TLC50F Peltier effect temperature controller. As presented as a function of wavenumber, the fluorescence intensities are multiplied by the square of the wavelength in order to compensate for the fixed (in wavelength units) spectral bandpass of the emission spectrograph.[23] The absorption and fluorescence instruments are controlled by LabVIEW (National Instruments) programs.

3. Results

Figure 4 shows a series of fluorescence emission spectra obtained from ZnCytc preparations at 22 °C as the excitation wavenumber is tuned over the absorption spectrum from the Q-band region to the Soret band region. The spectra show the

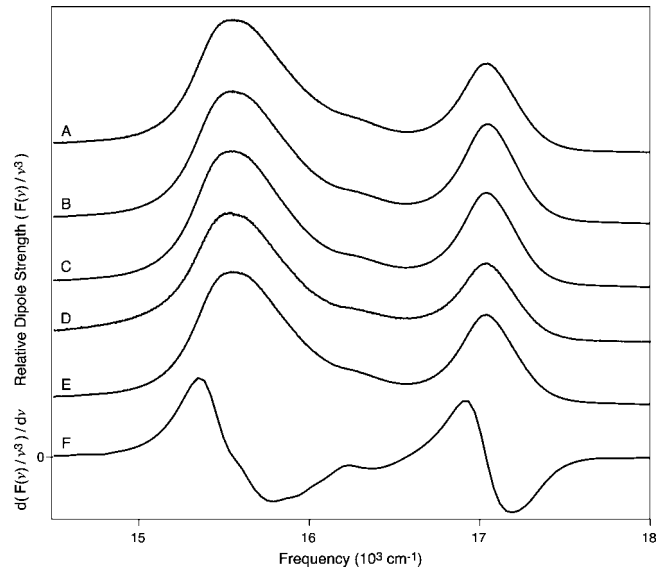

Figure 4. Continuous-wave fluorescence emission spectra from ZnCytc at 22 °C with the excitation source tuned to a series of wavelengths: (A) 380, (B) 420, (C) 427.5, (D) 440, and (E) 530 nm. The spectra are plotted with arbitrary scaling of the ordinate as the dipole strength, $F(\upsilon)/\upsilon^3$, as a function of the emission wavenumber, υ. Spectrum F shows the first derivative of the 530 nm spectrum (E), $\mathrm{d}(F(\upsilon)/\upsilon_3)/\mathrm{d}\upsilon$.

emission range spanned by the 0−0 and 0−1 vibronic peaks. As the excitation wavenumber is tuned, the intensity of the 0−0 peak (F_{0-0}) oscillates with respect to that of the 0−1 peak (F_{0-1}), which is always the stronger of the two, and there is a barely discernible red/blue/red oscillatory shift of the overall spectrum with respect to the emission wavenumber axis. These trends are presented in detail in Figure 5, which compares the dependence on the excitation wavenumber of the integrated fluorescence Stokes shift, plotted here as the wavenumber of the 0−0 peak maximum (υ_{0-0}), the F_{0-1}/F_{0-0} intensity ratio, and the line width ($\Delta\upsilon_{0-0}$), plotted as the half-width at half-maximum. The plotted abscissa, $\upsilon_{ex} - \upsilon_{0-0}$, the difference between the excitation wavenumber and the wavenumber for the 0−0 transition, where the absorption and fluorescence dipole strength spectra cross (see Figure 1), corresponds to the vibrational energy that is received by the protein structure at the chosen excitation wavenumber. In order to measure the plotted spectral parameters precisely, the wavenumbers for the maxima of the 0−1 and 0−0 peaks were estimated using the first and second zero crossings of the first-derivative spectrum (see Figure 4F for an example). The first-derivative spectrum was calculated after the fluorescence spectrum was smoothed by a smoothing spline routine. The F_{0-1}/F_{0-0} ratio was determined directly from the intensities at the two maxima. Lastly, $\Delta\upsilon_{0-0}$ was determined using the wavenumbers of the 0−0 maximum and the half-maximum on the blue side of the peak. This choice avoids the congested region between the 0−0 and 0−1 peaks. These measurements were performed either by a Matlab script or manually with the Igor Pro (Wavemetrics) program.

Aside from a small peak to the blue centered at 1350 cm^{-1}, Figure 5a shows that the fluorescence Stokes shift remains essentially constant at the value observed with excitation at the wavenumber of the 0−0 transition in the Q band until a vibrational excitation of 4400 cm^{-1} is reached. The 0−0 peak then exhibits a relatively sharp steplike shift of about 5 cm^{-1} to lower energy. The midpoint of the red shift is observed at an excitation energy of 5000 cm^{-1}. (These excitation wavenumber

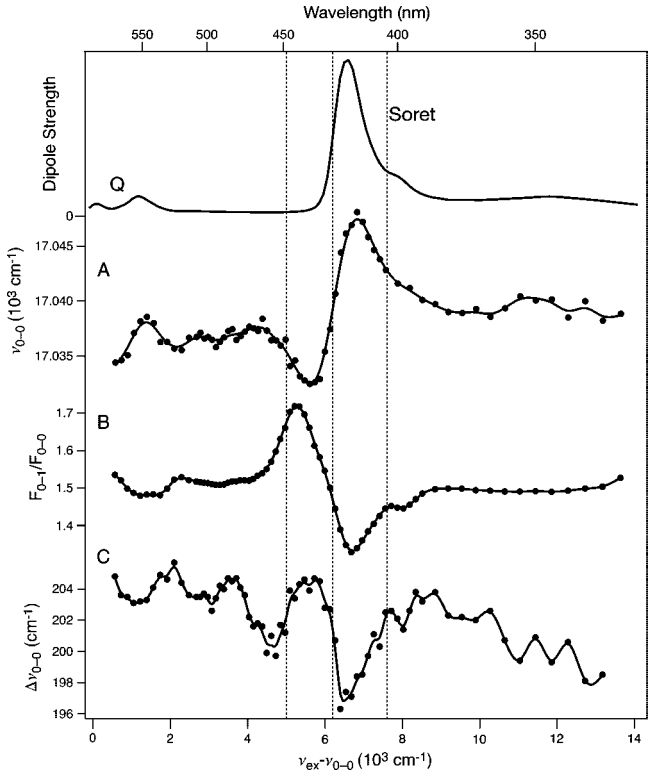

Figure 5. Dependence of the fluorescence spectrum from ZnCytc at 22 °C on the intramolecular vibrational excitation: (A) the integrated Stokes shift, as determined by the wavenumber of the 0−0 peak maximum, ν_{0-0}; (B) ratio of the dipole strengths of the 0−1 and 0−0 peaks, F_{0-1}/F_{0-0}; and (C) the half-width at half-maximum of the 0−0 peak, $\Delta\nu_{0-0}$. The curves drawn through the plotted data points were obained from a smoothing spline routine. The plotted abscissa is the intramolecular vibrational excitation, $\nu_{ex} - \nu_{0-0}$, the difference between the excitation wavenumber and that of the 0−0 vibronic transition (see Figure 1). At the top of the figure, the absorption dipole strength spectrum (see Figure 1) is plotted with respect to the same abscissa scale, and the corresponding excitation wavelength is marked on the top of the frame. The vertical dashed lines mark the excitation energies corresponding to apparent activation enthalpies for three protein-unfolding transition, which were estimated from the midpoints of the transitions in the integrated Stokes shift (A). These energies are listed in Table 1.

TABLE 1: Apparent Enthalpies of Activation for Protein Structural Transitions in ZnCytc and from the Midpoints of Steps in the Excitation Wavenumber Profile for the Integrated Fluorescence Stokes Shift (ν_{0-0}) (See Figures 5 and 8)

transition	direction of shift	ZnCytc	fbCytc1
1	red	5000 cm^{-1} (60 kJ/mol)	600 cm^{-1} (7.2 kJ/mol)[a]
2	blue	6200 cm^{-1} (74 kJ/mol)	1500 cm^{-1} (18 kJ/mol)
3	red	7600 cm^{-1} (91 kJ/mol)	2500 cm^{-1} (30 kJ/mol)

[a] Upper limit for transition midpoint.

estimates have uncertainties on the order of ±100 cm^{-1}.) A second step transition of the 0−0 peak then occurs to the blue; the midpoint of this 15 cm^{-1} transition is observed at 6200 cm^{-1}. Following this blue shift, the 0−0 peak exhibits a 8 cm^{-1} red shift with a midpoint at 7600 cm^{-1}. At higher excitation wavenumbers, the spectrum exhibits a broad peak to the blue with a 2 cm^{-1} shift centered at 11 400 cm^{-1}.

The midpoints of the three main step transitions observed in the fluorescence Stokes shift are listed in Table 1. These transitions are mirrored by steps in the F_{0-1}/F_{0-0} ratio (see Figure 5b), but the latter's midpoints are reached about 200 cm^{-1} earlier. A somewhat more complicated structure is exhibited by the excitation wavenumber profile of the line width $\Delta\nu_{0-0}$ (see Figure 5c). The shift of the spectrum to the red centered at 5000 cm^{-1} is preceded by a significant spectral narrowing; as the spectrum completes the red shift, the spectrum returns to its initial line width. The subsequent blue shift centered at 6200 cm^{-1} is accompanied by a narrowing that is larger than that observed in the initial red shift. The final red shift of the spectrum at 7600 cm^{-1} is accompanied by a broadening of the spectrum back to nearly its initial line width. An overall line-narrowing trend is observed, however, as the excitation wavenumber is scanned over the range spanned by the three Stokes shift transitions. Note that while the line width changes correspond only to a few percent of the overall line width, they are very well correlated with the transitions in the Stokes shift and in the F_{0-1}/F_{0-0} ratio.

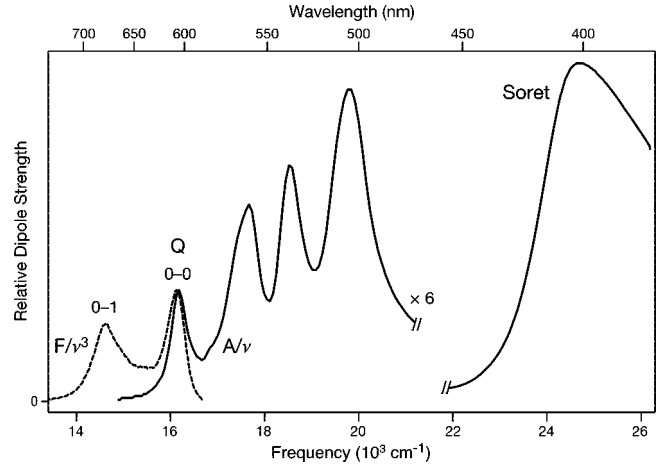

Figure 6. Continuous-wave absorption (A/ν, solid curve) and fluorescence (F/ν^3, dashed curve) dipole strength spectra from metal-free (free-base) cytochrome *c* (fbCytc) at 22 °C. The fluorescence spectrum was recorded with the excitation monochromator tuned to the wavenumber of the 0−0 vibronic transition, where the absorption and fluorescence dipole strength spectra cross. The 0−0 and 0−1 peaks in the absorption and fluorescence spectra are marked.

Figure 6 shows the absorption and fluorescence dipole strength spectra from fbCytc at 22 °C. The fluorescence spectrum is comparable in appearance to that of ZnCytc in having two vibronic peaks that are labeled 0−1 and 0−0 in wavenumber order. In contrast, the Q-band region of the absorption spectrum is split into four vibronic peaks, two each for the Q_x and Q_y states of the porphyrin macrocycle. This splitting arises upon demetalation when two of the four pyrrolic nitrogen atoms are protonated.[24] The fluorescence spectrum is mirror symmetric with respect to the lower energy (Q_y) band, so an absorption transition to the Q_x state is followed by nonradiative decay to the Q_y state. A lower limit for the optical reorganization energy for fbCytc can be estimated[25] as one-half the shift in energy between the 0−0 peaks in the fluorescence and absorption spectra, 37.5 cm^{-1}. In comparison, the optical reorganization energy for ZnCytc, 145 cm^{-1} (see Figure 1), was obtained previously using the same method.[12]

Figure 7 shows an excitation wavelength series of fluorescence spectra from fbCytc preparations at 22 °C. The F_{0-1}/F_{0-0} intensity ratio shows much smaller oscillations than was observed with ZnCytc (see Figure 4), but it is apparent that a substantial blue shift of the fluorescence spectrum occurs with a low vibrational excitation energy (compare the 550 and 570 nm spectra, Figures 7D,E). As the excitation wavenumber is

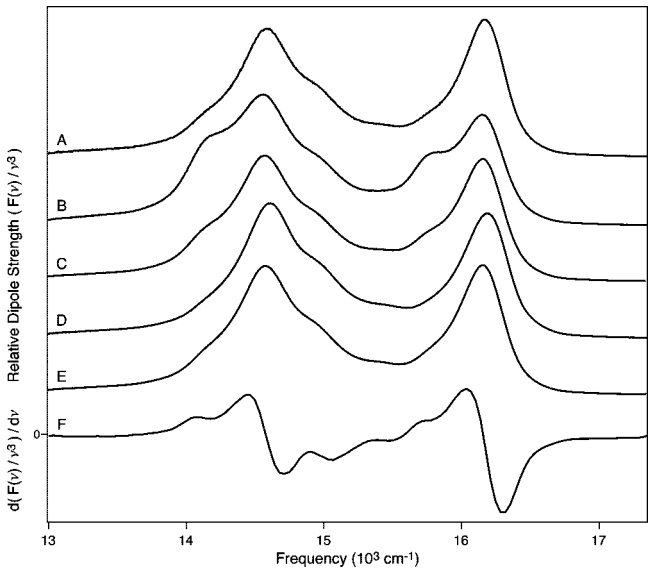

Figure 7. Continuous-wave fluorescnce emission spectra from fbCytc at 22 °C with the excitation source turned to a series of wavelengths: (A) 405, (B) 430, (C) 505, (D) 550, and (E) 570 nm. The spectra are plotted with arbitrary scaling of the ordinate as the dipole strength, $F(\upsilon)/\upsilon^3$, as a function of the emission wavenumber, υ. Spectrum F shows the first derivative of the 570 nm spectrum (E), $\mathrm{d}(F(\upsilon)/\upsilon^3)/\mathrm{d}\upsilon$.

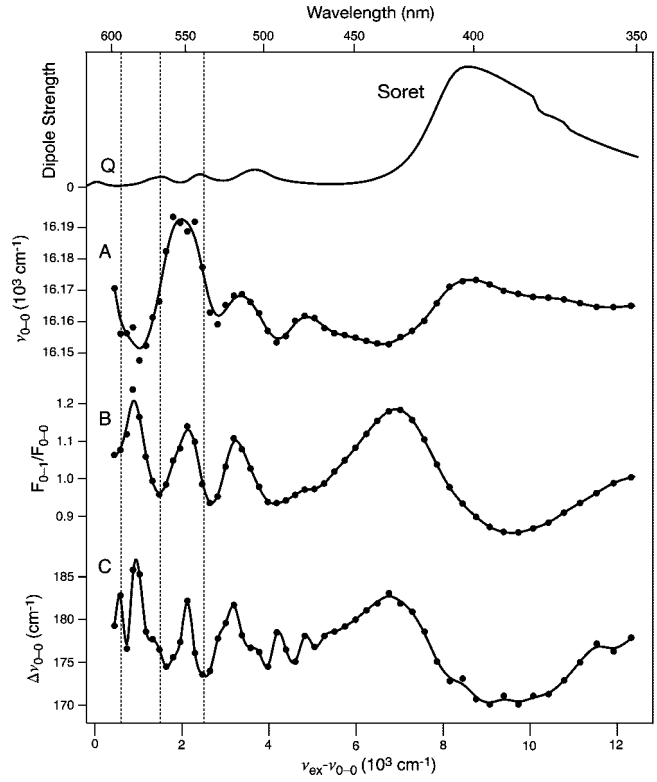

Figure 8. Dependence of the fluorescence spectrum from fbCytc at 22 °C on the intramolecular vibrational excitation: (A) the integrated Stokes shift, as determined by the wavenumber of the 0−0 peak maximum, υ_{0-0}; (B) ratio of the dipole strengths of the 0−1 and 0−0 peaks, F_{0-1}/F_{0-0}; and (C) the half-width at half-maximum of the 0−0 peak, $\Delta\upsilon_{0-0}$. The curves drawn through the plotted data points were obtained from a smoothing spline routine. The plotted abscissa is the intramolecular vibrational excitation, $\upsilon_{ex} - \upsilon_{0-0}$, the difference between the excitation wavenumber and that of the 0−0 vibronic transition (see Figure 6). At the top of the figure, the absorption dipole strength spectrum (see Figure 6) is plotted with respect to the same abscissa scale, and the corresponding excitation wavelength is marked on the top of the frame. The vertical dashed lines mark the excitation energies corresponding to apparent activation enthalpies for three protein-unfolding transitions, which were estimated from the midpoints of the transitions in the integrated Stokes shift (A). These energies are listed in Table 1.

tuned into the Soret band region (Figures 7A−C), the fluorescence spectrum from fbCytc exhibits some additional, partially resolved vibronic structure especially on the red side of the 0−1 peak. In contrast, the fluorescence spectra from ZnCytc exhibit comparable line shapes across the whole range of excitation wavenumbers (see Figure 4).

Figure 8 shows the dependence on the excitation wavenumber in fbCytc preparations of the integrated Stokes shift (υ_{0-0}), the F_{0-1}/F_{0-0} ratio, and the $\Delta\upsilon_{0-0}$ line width. These parameters were measured using the same procedure used for the spectra from ZnCytc. Three step transitions are observed in υ_{0-0} but at significantly lower excitation energies than observed in ZnCytc (see Table 1). The midpoint of the initial red shift is observed at an excitation of 600 cm^{-1}, but it is possible that this transition is truncated since a flat region prior to the transition like that of ZnCytc (see Figure 5A) is not observed. The F_{0-1}/F_{0-0} ratio (Figure 8B) also exhibits an undulating pattern as the excitation wavelength is tuned, but the ratio is confined to a smaller range than in ZnCytc, 0.95−1.2. The structure in the ratio over the <3000 cm^{-1} range is shifted to the red by ∼1000 cm^{-1} compared to that in the υ_{0-0} trace (see Figure 8A). The excitation wavenumber profile of the fluorescence line width $\Delta\upsilon_{0-0}$ (Figure 8C) exhibits a sharp structure that is largely confined to the <3000 cm^{-1} region where the υ_{0-0} and F_{0-1}/F_{0-0} traces exhibit transitions. As in the case of ZnCytc, the fluorescence line width of fbCytc narrows in the excitation wavenumber regions that coincide with the midpoints of spectral shifts and broadens at the ends of shifts. This pattern ends in the Soret band region, where the line width trace more or less parallels the F_{0-1}/F_{0-0} trace. Again, as the excitation wavenumber is scanned to the blue, the overall trend is a modest narrowing of the fluorescence spectrum.

4. Discussion

The three transitions observed in the excitation wavenumber dependence of the fluorescence spectra from ZnCytc and fbCytc (Figures 5 and 8) evidence the transient formation of partially unfolded structures during the 0 to ∼15 ns time window spanned by the fluorescence emission. By monitoring the line shape and Stokes shift of the Q-band fluorescence spectrum as the excitation wavenumber is tuned, we exploit the intrinsic porphyrin as a solvatochromic probe of the structural dynamics that it triggers via IVR and/or radiationless decay of the excess vibronic energy above the S_1 state. The interpretation of the results we provide in the following depends crucially on the experimental design employed in this work. Owing to the use of dilute solutions, a low-intensity light source, and a Peltier effect sample temperature controller, the sample temperature remained constant as the excitation wavenumber was tuned. Further, the measured excitation wavenumber profiles are not dependent on the excitation light intensity (results not shown). Thus, the spectral transitions observed in these experiments do not arise from long-lived changes in the surrounding solvent temperature that are induced by scanning through structure in the absorption spectrum in the course of an experiment. Nevertheless, especially as the excitation wavenumber is scanned from the vibronic manifold of the S_1 state into that of the Soret band, where a range of electronic states S_n are populated, it is likely that the $S_n \rightarrow S_1$ internal conversion rate and the nature of the porphyrin's initial vibrational excitation

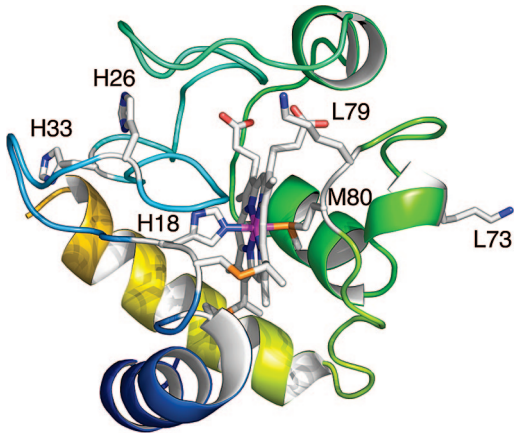

Figure 9. Structure of ferricytochrome *c* (FeCytc, pdb file 1HRC). The polypeptide backbone is displayed in a ribon representation. The side chains of the amino acids that are ligated to the Zn^{II} ion in the native structure of ZnCytc (H18 and M80) and those that are candidates for ligation in the partially unfolded states yielded by intramolecular vibrational excitation (the products of transitions 2 and 3 in Table 1) are indicated as stick structures.

are not constant. These effects may have an impact on the *rates* of the protein reactions, as discussed below, that will be obscured by our use of time-integrated spectral parameters.

Despite these limitations, the excitation wavenumber profiles discussed in this paper provide a basis for a subsequent series of studies using time-resolved fluorescence spectroscopy of the protein reactions that follow excitation near and above the three apparent activation barriers. The profiles exhibited by the line widths $\Delta\upsilon_{0-0}$ (see Figures 5c and 8c) are of particular significance because they indicate that discrete protein structures are generated as products as each activation barrier is surpassed. If the vibrational excitation delivered by the porphyrin produces only a local melting of the protein structure, the line width would be expected to broaden monotonically as a range of random structures is increasingly populated from the native state as the excitation wavenumber is scanned to the blue. Instead, the line width undergoes oscillatory transitions that are tightly correlated with the profiles exhibited by the integrated Stokes shift and the F_{0-1}/F_{0-0} ratio. The nature of the structural transitions that occur in ZnCytc and fbCytc can be inferred from the direction of the Stokes shift transition. Given a normal solvatochromic response arising from an ground-to-excited-state increase in the dipole moment of the chromophore, a shift of the spectrum to the red should be taken as an indication that the solvent environment of the porphyrin increases in polarity.[26]

A possible explanation for the lowest energy structural transition (see Table 1), then, is a reorganization that increases the exposure of the porphyrin to the surrounding aqueous phase. Because it lacks the metal−protein interactions along the axial direction (normal to the plane of the porphyrin), an especially low activation energy barrier would be expected in fbCytc for a change in structure that admits water molecules into the region surrounding the porphyrin through the aperture in the solvent-contact surface (see Figure 9). When compared to the optical reorganization energy, the Stokes shift associated with the first transition is much larger in fbCytc than in ZnCytc. This comparison suggests that this transition yields a greater degree of solvent exposure for the porphyrin in fbCytc than in ZnCytc.

The axial metal−ligand interactions in ZnCytc raise the height of the first barrier and increase the sharpness of the Stokes shift transition that accompanies its passage. As argued previously in our discussion of the vibronic structure in a series of picosecond time-resolved fluorescence spectra,[27] the F_{0-1}/F_{0-0} ratio in ZnCytc is a measure of the extent to which the Zn ion coordinates axial ligands.[28,29] A low F_{0-1}/F_{0-0} ratio is observed at the lowest excitation energies (and in the ground state, as judged from the absorption spectrum; see Figure 5) when both of the amino acids that serve as axial ligands to the Fe^{III} ion in the FeCytc structure, M80 and H18, are likely to be bound (see Figure 9). The resulting six-coordinate Zn^{II}−porphyrin complex is strained, and the first axial ligand to dissociate, M80, apparently departs on the 100 ps time scale even with excitation at the wavenumber of the 0−0 transition, at a net intramolecular vibrational excitation of 0 cm^{-1}.[27] Thus, the rapid change in the F_{0-1}/F_{0-0} ratio that accompanies the first Stokes shift transition reports a dramatic increase in the rate at which the second ligand, H18, dissociates from the Zn^{II} ion. We showed previously that the release of both axial ligands is rate limited by the external solvent viscosity; in effect, the Zn^{II}−porphyrin expands along the axial direction as the ligands depart, and the rate at which the protein structure accommodates this change in volume is limited by a *nonpolar* reorganization of the surrounding solvent.[27]

The second structural transition in ZnCytc and fbCytc, a shift of the fluorescence spectrum to the blue, describes an abrupt decrease in the polarity of the medium that surrounds the porphyrin. Blue shifts are also associated with the transition from the native structure to the acid-induced molten-globule state that is observed in the presence of salt and with the transition from the native state to the acid-denatured state.[30−34] The fluorescence spectrum also shifts to the blue when the protein unfolds thermally.[13] Recall that the magnitude of the *dynamic* Stokes shift to the blue observed with excitation at 420 nm in the time-resolved experiment exceeds 150 cm^{-1} (see Figure 2),[10] so a significant reorganization of the protein structure that is comparable to that incurred during the thermal unfolding transition is indicated by the Stokes shift transition shown in Figure 5. An even larger reorganization is indicated by the second Stokes shift transition observed in fbCytc (see Figure 8). In both systems, the protein structure apparently reorganizes in this transition so that the porphyrin is much more deeply embedded in the hydrophobic region of the protein.

In ZnCytc, the concomitant large decrease in the F_{0-1}/F_{0-0} ratio that accompanies the second Stokes shift transition indicates a significant reorganization of the folded protein to permit the binding of a different ligand to the Zn^{II} ion. Rebinding of the initially bound M80 and H18 ligands cannot be excluded arbitrarily, but the F_{0-1}/F_{0-0} ratio and υ_{0-0} reached at the end of the transition are different from those present initially at low excitation wavenumber, so is is likely that a different ligand has bound to the Zn^{II} ion. Figure 9 suggests several possible candidates for this binding event. Histidine residues H33 and H26 have been implicated as intermediates during the folding of FeCytc prior to the binding of M80 as an axial ligand.[18] The binding of H33 or H26 to the Zn^{II} ion in ZnCytc on either face of the porphyrin would require a substantial reorganization of the hydrophobic loop that lies between H18 and H33, so ligation of either amino acid might be accompanied by a blue shift of the fluorescence spectrum. A reorganization of the protein on the M80 side of the porphyrin such that the lysine residues L73 and L79[35] approach and bind to the Zn^{II} ion seems less reasonable because this hydrophilic part of the protein is directed to the surface of the protein in the native structure, so binding of L73 or L79 by the Zn^{II} ion might be expected to increase, rather than decrease, the polarity of the porphyrin binding region. The same might be said about a possible binding of a water

ligand to the Zn^{II} ion. These possibilities can be tested through the use of resonance Raman spectroscopy with Soret band excitation, which yields a spectrum that is sensitive to the nature of the axial ligands.[22,34,35]

The third structural transition in ZnCytc and fbCytc is associated with a shift of the fluorescence spectrum to the red. As argued for the first transition, such a shift is probably associated with an increased exposure of the porphyrin to the surrounding bulk solvent. In fbCytc, this is a large red shift that is comparable in range to that of the blue shift in the second transition; in ZnCytc, the red shift is comparable to that of the first transition, so a net shift to the blue is encountered from the native state. These observations argue again that the metal−ligand interactions control the structure in ZnCytc. We suggest that fbCytc moves in the third transition from a state that resembles a molten-globule state in having a well-defined hydrophobic core to one that is increasingly disordered as the excitation energy increases; the undulations in the integrated Stokes shift that are observed at still higher excitation energies might arise from additional reorganization of a largely unfolded structure. In ZnCytc, the associated change in the F_{0-1}/F_{0-0} ratio suggests that the third transition is likely to involve exchange of the amino acid that replaced H18 during the second transition for another amino acid, such as H33, or for a water molecule.

The preceding discussion raises the possibility that the three partially unfolded states detected in ZnCytc might be comparable to the rate-limiting late intermediates along the *folding* pathway for ferricytochrome *c* (FeCytc) that involve axial ligand-exchange reactions. The folding pathway involves formation of a H18−Fe−water intermediate followed by a rate-limiting exchange of the water molecule for the native M80 ligand.[18,36,37] The activation enthalpy for this step determined from its temperature dependence, 75 kJ/mol,[36] is about the same as the apparent activation enthalpies from the native state for the formation of the three partially unfolded states in ZnCytc (see Table 1). A somewhat lower activation enthalpy, 31.4 kJ/mol, was determined by Roder and co-workers for the initial formation of a condensed, partially folded state from the denatured state.[19] The activation enthalpies for the three states detected in fbCytc are lower still. These comparisons suggest that the absence of the metal ion in fbCytc leads to a relatively unstable molecule even under the solvent conditions that favor the native state of ZnCytc or FeCytc.

Note that the initial sequence of shifts of the continuous-wave fluorescence spectrum to the red and then to the blue that occur as the excitation source is tuned mirrors the directionality of the *dynamic* Stokes shift response observed with excitation of ZnCytc at 420 nm, which lies just past the wavenumber of the maximum of the blue shift that follows the second barrier (see Figures 2 and 5). This comparison strongly suggests that the sequence of activation barriers detected in the present experiments marks an increasing displacement from the native structure along an unfolding pathway (see Figure 10). Rather than moving from the native state directly to the intermediate state that lies after the second barrier, the 420 nm excitation drives the system first to the red-shifted state that is produced at excitation energies above the first barrier. At present, we have not recorded the time-resolved fluorescence response of ZnCytc with excitation above the third barrier, but we suggest that the final red-shifted state would be populated after the system moves sequentially from the native state through the first and second intermediate states. Note that the dynamic Stokes shift with 420 nm excitation apparently exhibits a very weak, final component toward the red on the >10 ns time scale (which is not shown in Figure 2). In 50% methanol, where the overall response is several times faster than in water, the dynamic Stokes shift observed with 420 nm excitation contains a final component that yields a red-shifted state after passing through a blue-shifted state; in this case, an initial red shift is not observed perhaps because it occurs during the 0−100 ps instrument-response dead time. These observations indicate that the three barriers are lowered from those in water owing to the decreased external solvent polarity according to the hydrophobic effect.[10]

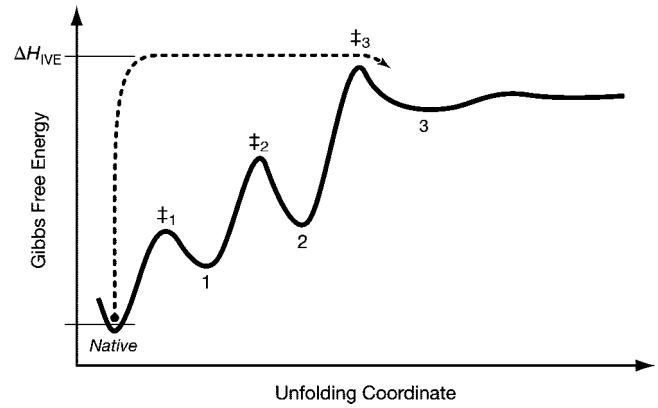

Figure 10. Gibbs free energy/protein-unfolding-coordinate profile for ZnCytc and fbCytc, showing schematically the ordering of intermediates and the intervening activation barriers (see Table 1) between the native state and the partially unfolded states. The dashed arrow marks the process that is driven by an intramolecular vibrational excitation (IVE) above the third transition-state barrier, $\Delta H_{IVE} > \Delta G_3^{\ddagger}$: after the vertical ($\Delta G \approx \Delta H_{IVE}$) excitation, the system propagates sequentially through the intermediates (1 and 2) on the way to the final state (3).

The finding that the fluorescence line width, $\Delta\nu_{0-0}$, oscillates in synchrony with the integrated Stokes shift and with the F_{0-1}/F_{0-0} ratio is inconsistent with the population of the intermediate states according to a Maxwell−Boltzmann distribution over all of the folding states accessible at a given excitation wavenumber. The line width would be expected then to exhibit a general broadening with increasing excitation wavenumber owing to the superposition of the spectra from each state and the weighting by the populations in each. In contrast, in addition to the oscillations noted above, the line width in fbCytc and ZnCytc exhibits a narrowing trend as the excitation wavenumber is tuned across the three transitions. These observations imply that the partially unfolded states are formed along the pathway from the native state in a sequential manner so that state with the largest possible entropy is specifically formed. But the product state has a finite lifetime; after the residual enthalpy of activation provided by the porphyrin has been dissipated collisionally to the surrounding solvent, the most probable state returns to being the native state. We expect, then, that the protein will eventually refold to form the native structure that was present prior to the absorption of the photon.

The reader should keep in mind that the time-integrated fluorescence spectrum is sensitive primarily to structural dynamics during the first few nanoseconds after the vibrational excitation since the fluorescence lifetime of ZnCytc and fbCytc is ~2 ns; the response functions measured in our earlier work reach out to 5 or 6 times the fluorescence lifetime.[10,12,27] An experiment capable of following the protein structural changes out to the milliseconds time scale is required to determine the fate of these transient structures. Nevertheless, the ligand-exchange reactions that we detect in ZnCytc imply that substantial reorganizations of the protein structure occur during the fluorescence time window. If these (or analogous) reactions

were triggered under the ambient bath conditions, say by a small temperature jump or by a rapid-flow mixing event from the denatured state, one would expect them to extend over the microseconds−milliseconds time scale. We suggest, then, that the rate at which the protein evolves structurally after an intramolecular vibrational excitation from the porphyrin is orders of magnitude faster than associated with a thermal excitation.

The results raise a number of new prospects for the study of protein *refolding* dynamics. Because it is apparently possible to prepare with energy selectivity a range of partially unfolded states on a time scale that is short compared to the rate that proteins evolve thermally, an intramolecular vibrational excitation can be used as a trigger in kinetic studies of the thermalized folding trajectories that follow on a longer time scale. Further, because the rate of IVR is fast compared to the rate at which collisions with the surrounding solvent dissipates the intramolecular vibrational excitation, it should not be necessary to employ chromophores that are protected from the solvent. By varying the temperature of the surrounding solvent, the refolding of a partially unfolded state can be studied so as to obtain Arrhenius activation parameters. By varying the composition of the surrounding solvent, the effect of solvent friction or polarity on the refolding dynamics can be studied directly. These experiments will permit the characterization of protein dynamics far from equilibrium without the usual constraints of the initial folding state.

Acknowledgment. This work was supported by the National Science Foundation Biomolecular Systems Cluster/Molecular Biophysics program under Grants MCB-009120 and MCB-050002. Additional support for instrumentation was provided by the Michigan Structural Biology Center at Michigan State University, which is supported by the Michigan Life Sciences Corridor. We thank Jana Grochol for the Matlab script that was used in the analysis of the fluorescence spectra.

References and Notes

(1) Leopold, P. E.; Montal, M.; Onuchic, J. N. Protein folding funnels: a kinetic approach to the sequence-structure relationship. *Proc. Natl. Acad. Sci. U.S.A.* **1992**, *89*, 8721–8725.

(2) Sali, A.; Shakhnovich, E.; Karplus, M. How does a protein fold. *Nature (London)* **1994**, *369*, 248–251.

(3) Bryngelson, J. D.; Wolynes, P. G. Spin glasses and the statistical mechanics of protein folding. *Proc. Natl. Acad. Sci. U.S.A.* **1987**, *84*, 7524–7528.

(4) Frauenfelder, H.; Sligar, S. G.; Wolynes, P. G. The energy landscapes and motions of proteins. *Science* **1991**, *254*, 1598–1603.

(5) Onuchic, J. N.; Luthey-Schulten, Z.; Wolynes, P. G. Theory of protein folding: The energy landscape perspective. *Annu. Rev. Phys. Chem.* **1997**, *48*, 545–600.

(6) Dill, K. A.; Chan, H. S. From Levinthal to pathways to funnels. *Nat. Struct. Biol.* **1997**, *4*, 10–19.

(7) Chan, H. S.; Dill, K. A. Protein folding in the landscape perspective: Chevron plots and Non-Arrhenius kinetics. *Proteins: Struct. Funct. Genet.* **1998**, *30*, 2–33.

(8) Shea, J.-E.; Brooks, C. L., III. From folding theories to folding proteins: a review and assessment of simulation studies of protein folding and unfolding. *Annu. Rev. Phys. Chem.* **2001**, *52*, 499–535.

(9) Dill, K. A. Polymer principles and protein folding. *Protein Sci.* **1999**, *8*, 1166–1180.

(10) Lampa-Pastirk, S.; Beck, W. F. Intramolecular vibrational preparation of the unfolding transition state of Zn^{II}-substituted cytochrome *c*. *J. Phys. Chem. B* **2006**, *110*, 22971–22974.

(11) Stratt, R. M.; Maroncelli, M. Nonreactive dynamics in solution: the emerging molecular view of solvation dynamics and vibrational relaxation. *J. Phys. Chem.* **1996**, *100*, 12981–12996.

(12) Lampa-Pastirk, S.; Beck, W. F. Polar solvation dynamics in Zn(II)-substituted cytochrome *c*: diffusive sampling of the energy landscape in the hydrophobic core and solvent-contact layer. *J. Phys. Chem. B* **2004**, *108*, 16288–16294.

(13) Lesch, H.; Stadlbauer, H.; Friedrich, J.; Vanderkooi, J. M. Stability diagram and unfolding of modified cytochrome *c*: what happens in the transformation regime. *Biophys. J.* **2002**, *82*, 1644–1653.

(14) Miller, R. J. D. Vibrational energy relaxation and structural dynamics of heme proteins. *Annu. Rev. Phys. Chem.* **1991**, *42*, 581–614.

(15) Lian, T.; Locke, B.; Kholodenko, Y.; Hochstrasser, R. M. Energy flow from solute to solvent probed by femtosecond IR spectroscopy: Malachite Green and heme protein solutions. *J. Phys. Chem.* **1994**, *98*, 11648–11656.

(16) Owrutsky, J. C.; Raftery, D.; Hochstrasser, R. M. Vibrational relaxation dynamics in solution. *Annu. Rev. Phys. Chem.* **1994**, *45*, 519–555.

(17) Genberg, L.; Heisel, F.; McLendon, G.; Miller, R. J. D. Vibrational energy relaxation processes in heme proteins: model systems of vibrational energy dispersion in disordered systems. *J. Phys. Chem.* **1987**, *91*, 5521–5524.

(18) Yeh, S.-R.; Rousseau, D. L. Folding intermediates in cytochrome *c*. *Nat. Struct. Biol.* **1998**, *5*, 222–228.

(19) Shastry, M. C. R.; Roder, H. Evidence for barrier-limited protein folding kinetics on the microsecond time scale. *Nat. Struct. Biol.* **1998**, *5*, 385–392.

(20) Vanderkooi, J. M.; Adar, F.; Ericińska, M. Metallocytochromes *c:* Characterization of electronic absorption and emission spectra of Sn^{4+} and Zn^{2+} cytochromes *c*. *Eur. J. Biochem.* **1976**, *64*, 381–387.

(21) Elias, H.; Chou, M. H.; Winkler, J. R. Electron-transfer kinetics of Zn-substituted cytochrome *c* and its $Ru(NH_3)_5$(Histidine-33) derivative. *J. Am. Chem. Soc.* **1988**, *110*, 429–434.

(22) Ye, S.; Shen, C.; Cotton, T. M.; Kostić, N. M. Characterization of zinc-substituted cytochrome *c* by circular dichroism and resonance Raman spectroscopic methods. *J. Inorg. Biochem.* **1997**, *65*, 219–226.

(23) Lakowicz, J. R. *Principles of Fluorescence Spectroscopy*, 2nd ed.; Kluwer Academic/Plenum Publishers: New York, 1999.

(24) Gouterman, M. Optical spectra and electronic structure of porphyrins and related rings. In *The Porphyrins*; Dolphin, D., Ed.; Academic Press: New York, 1978; Vol. 3, pp 1−159.

(25) Jordanides, X. J.; Lang, M. J.; Song, X.; Fleming, G. R. Solvation dynamics in protein environments studied by photon echo spectroscopy. *J. Phys. Chem. B* **1999**, *103*, 7995–8005.

(26) Bayliss, N. S.; McRae, E. G. Solvent effects in organic spectra: dipole forces and the Franck-Condon principle. *J. Phys. Chem.* **1954**, *58*, 1002–1006.

(27) Lampa-Pastirk, S.; Lafuente, R. C.; Beck, W. F. Excited-state axial-ligand photodissociation and nonpolar protein-matrix reorganization in Zn(II)-substituted cytochrome *c*. *J. Phys. Chem. B* **2004**, *108*, 12602–12607.

(28) Nappa, M.; Valentine, J. S. The influence of axial ligands on metalloporphyrin visible absorption spectra. Complexes of tetraphenylporphynatozinc. *J. Am. Chem. Soc.* **1978**, *100*, 5075–5080.

(29) Humphry-Baker, R.; Kalyanasundaram, K. Influence of axial ligation on the fluorescence of tetrakisphenylporphyrins. *J. Photochem.* **1985**, *31*, 105–112.

(30) Ohgushi, M.; Wada, A. "Molten-globule state"—a compact form of globular proteins with mobile side-chains. *FEBS Lett.* **1983**, *164*, 21–24.

(31) Jeng, M.-F.; Englander, S. W.; Elöve, G. A.; Wand, A. J.; Roder, H. Structural description of acid-denatured cytochrome *c* by hydrogen exchange and 2D NMR. *Biochemistry* **1990**, *29*, 10433–10437.

(32) Hamada, D.; Kuroda, Y.; Kataoka, M.; Aimoto, S.; Yoshimura, T.; Goto, Y. Role of heme axial ligands in the conformational stability of the native and molten globule states of horse cytochrome *c*. *J. Mol. Biol.* **1996**, *256*, 172–186.

(33) Lyubovitsky, J. G.; Gray, H. B.; Winkler, J. R. Structural features of the cytochrome *c* molten globule revealed by fluorescence energy transfer kinetics. *J. Am. Chem. Soc.* **2002**, *124*, 14840–14841.

(34) Oellerich, S.; Wackerbarth, H.; Hildebrandt, P. Spectroscopic characterization of nonnative conformational states of cytochrome *c*. *J. Phys. Chem. B* **2002**, *106*, 6566–6580.

(35) Döpner, S.; Hildebrandt, P.; Rosell, F. I.; Mauk, A. G. Alkaline conformational transitions of ferricytochrome *c* studied by resonance Raman spectroscopy. *J. Am. Chem. Soc.* **1998**, *120*, 11246–11255.

(36) Yeh, S.-R.; Takahashi, S.; Fan, B.; Rousseau, D. L. Ligand exchange during cytochrome *c* folding. *Nat. Struct. Biol.* **1997**, *4*, 44–50.

(37) Gianni, S.; Travaglini-Allocateli, C.; Cutruzzolla, F.; Brunori, M.; Shastry, M. C. R.; Roder, H. Parallel pathways in cytochrome *c*(551) folding. *J. Mol. Biol.* **2003**, *330*, 1145–1152.

JP803756N